NASA Technical Paper 1943

November 1981

Analytic Investigation of Effect of End-Wall Contouring on Stator Performance

Robert J. Boyle,
Harold E. Rholik,
and Louis J. Goldman

NASA

NASA
Technical
Paper
1943

1981

Analytic Investigation of Effect of End-Wall Contouring on Stator Performance

Robert J. Boyle,
Harold E. Rholik,
and Louis J. Goldman
Lewis Research Center
Cleveland, Ohio

NASA
National Aeronautics and Space Administration
Scientific and Technical Information Branch

Summary

The performance of various contour geometries were evaluated to help understand why a contoured stator improves performance. These contours had an inlet area larger than the exit area. A quasi-three-dimensional analysis was used. The results of a hub-shroud midchannel stream surface analysis were used to obtain solutions on blade-to-blade surfaces. Solutions were obtained for several streamlines from the hub to the tip. Surface velocities were used to calculate profile and end-wall losses. Comparing analytic results with previously published experimental data showed reasonably good agreement.

The effect of contour geometry for a highly loaded stator was analytically investigated. Inlet- to exit-passage-height ratio, contour length, and location of the contour significantly affected stator performance. Efficiency increased with increased passage-height ratio until a ratio of 1.2 was reached. The gain was 0.8 percentage point over the efficiency of 96.4 percent for the cylindrical end-wall case. This corresponded to a 22-percent reduction in stator losses. The tip radius was kept constant for the first half of the chord. Longer contours resulted in less efficiency gain, while shorter contours resulted in loss of tangential momentum. Terminating the contour upstream of the trailing edge yielded smaller efficiency gains. The contour shape and the hub to tip radius ratio were found to have little effect for the particular cases investigated. When end-wall contouring was examined for a lightly loaded stator, the improvement was significantly less.

To understand how end-wall contouring would affect secondary flow, comparisons were made for surface velocities at different radial positions and for blade surface static pressures. Where the flow is turned rapidly, surface velocities were reduced. Therefore, the driving force for cross-channel flows on the end-walls was reduced. Pressure distribution on the blade suction surface showed a reduced driving force for radial secondary flows.

Introduction

In the quest for improved turbine performance, one of the tools which may be used is contouring the end wall of an axial stator. This is done using a noncylindrical end wall with the passage area greater at the inlet than at the exit. The outer end wall is contoured to accomodate this area change. The amount of area change, the length of the contour, and its location within the passage are important considerations in the contour design. Contouring the end wall has the potential for reducing stator losses in two ways. First, the boundary layer growth is modified due to the lower velocity at the inlet and during most of the turning. Second, there is a reduction in secondary losses by virtue of the reduced pressure gradient both across the channel and in the radial direction. The low velocity turning reduces the cross-channel pressure gradient, and contouring the outer wall reduces the radial pressure gradient.

There have been several experimental studies showing the benefits of contoured end walls. References 1 to 4 showed improved performance due to end wall contouring. Reference 1 gives parametric data to determine contour geometry to achieve maximum gains for the blades tested. Reference 4 gives data for a highly turned stator designed for an advanced core engine.

The objective of the study reported herein was to gain an understanding of the factors that contribute to reduced losses when using contoured end walls as shown by the experimental studies. The approach involved the calculation of boundary-layer losses for different contour geometries and the examination of the static-pressure distributions that drive secondary flows. To establish the appropriateness of the analytic procedure, comparisons are made with the experimental results of reference 4. A quasi-three-dimensional flow analysis was used. The flow properties on the hub-shroud, midchannel, stream surface were first determined using the computer code described in reference 5. The results of this analysis were then used to calculate flow properties in the blade-to-blade direction for several stream surfaces using the computer code described in reference 6. The resulting velocity distributions were used in a boundary-layer analysis (ref. 7) to determine profile and end-wall losses.

In addition to the comparison with experimental data, the effect of different contour geometries on stator performance was examined analytically. To understand how end-wall contouring affects the driving forces for secondary flows, a single contour was examined in detail.

Symbols

- A axial aspect ratio at stator exit
- a length of initial constant area section, percent of chord
- b length of contour, percent of chord
- h ratio of passage inlet height to passage exit height
- M^* critical velocity ratio

Method of Analysis

Figure 1 shows the geometry of a contoured end-wall configuration. The blade passage is bounded by two blades, a cylindrical hub, and a contoured tip. The tip contour is axisymmetric rather than being alined with the direction of the flow. In the three-dimensional sketch the contour appears to be fairly shallow. This is the result of the large amount of turning in the passage. The projection shows a rapid change in end-wall radius in the last half of the chord. The analysis was done by specifying conditions upstream of the blade and the whirl, which varied with radius, a distance downstream of the trailing edge.

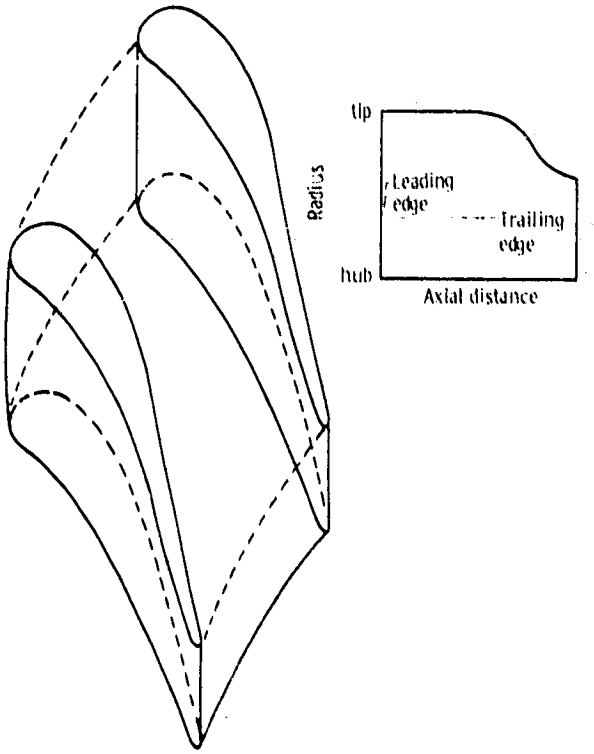

Figure 1. - Schematic of blade passage with a contoured tip.

An iterative procedure was used to determine stator performance. In the procedure an initial estimate was made for the downstream whirl. With this estimate the flow-field velocity distribution was determined using a quasi-three-dimensional inviscid analysis. Once the velocity distribution was found, a boundary-layer analysis was done to determine momentum thicknesses on both the blade surfaces and end walls. A check was made of the static-pressure difference across the blade near the trailing edge. When this difference did not approach zero, the estimate of the downstream whirl distribution was changed, and the procedure repeated.

The quasi-three-dimensional flow analysis was accomplished using the results of two flow programs. Each program analyzes the flow in a single plane. The first program, MERIDL (described in ref. 5) calculates flow properties on the hub-shroud midchannel stream surface. One of the results of this program is the stream-sheet thickness necessary to pass 1 percent of the total flow on a blade-to-blade surface of revolution. The thickness varied as a function of radius and axial distance. The calculated thicknesses were used as part of the input to the second flow analysis program. This program, TSONIC (described in ref. 6) calculates flow properties on blade-to-blade surfaces. Typically, the surfaces were the hub, tip, and three additional streamlines within the passage. The analysis was not fully three dimensional. This was because the stream-sheet thickness necessary to pass 1 percent of the flow could not vary in the blade-to-blade direction, and all surfaces on which the blade-to-blade analysis was done were surfaces of revolution.

The surface velocities were used in a boundary-layer analysis to calculate displacement and momentum thicknesses for both blade surface and end-wall streamlines. This boundary-layer analysis assumed turbulent compressible flow and was done using the program BLAYER described in reference 7. The boundary-layer calculations were done for each iteration. The iteration procedure was stopped when the static-pressures on each side of the blade were approximately equal near the trailing edge. The boundary-layer analysis provided information regarding the uncertainty in the losses as the iterations progressed. Generally, several iterations were required. The change in the static-pressure difference was small for the final few iterations. Since the stator loss was proportional to the momentum thickness near the trailing edge, the variation in momentum thickness for the last few iterations gave an estimate of the uncertainty in stator loss.

The total calculated loss for each case was taken as the sum of the profile loss and end-wall loss. The profile loss was calculated using the procedure

described in reference 8 for calculating the aftermixed efficiency based on kinetic energy. This procedure involved integration in the radial direction. At each radius the required information was obtained using the analysis given in reference 9 to determine mixed out losses. The end-wall loss was treated as being analogous to the profile loss for individual streamlines. For the end-wall loss the first streamline is at the suction surface, and the last one is at the pressure surface. The loss for each streamline required boundary-layer data from the hub and shroud surfaces. The end-wall loss was calculated by averaging the loss for each of five streamlines.

After the final flow field iteration, the static pressure distributions on the blade surfaces were determined. The static-pressure distribution on each surface was obtained from the local total pressure and the blade surface velocities for each radial streamline. Because pressure loss was included as part of the flow analysis, the total pressure decreased with distance along the streamline.

Results and Discussion

Comparison of Experimental and Predicted Results

To evaluate the appropriateness of the analytic approach a comparison was made with experimental data. The experimental results are presented in reference 4, where two tests were discussed. In the first a planar cascade was tested, and in the second, one end-wall was contoured. Two analytic cases were run to compare with these experimental data. The analysis used the same passage geometry as the experimental cascade, and a large radius was used to simulate a planar cascade.

Figure 2 gives a comparison of the experimental and predicted flow angles for the contoured end-wall case as a function of the distance from hub to tip. The experimental data were mass averaged at each radial location, while the predicted flow angle was calculated by the program MERIDL. These data are compared at approximately one-third of an axial chord downstream of the trailing edge. The experimental data were measured with the zero reference in the tangential direction, which was 90° from the inlet flow direction. Analytically the flow is not uniformly turned at this distance downstream of the trailing edge. At this axial location the program TSONIC predicted a variation of about 4° in the blade-to-blade direction at each radial streamline. At each radius the average angle calculated from the TSONIC results agreed well with the midchannel angle given by MERIDL.

Figure 3 gives a comparison of experimental and predicted blade-surface pressures at four spanwise locations. These locations are designated by their percent of exit span. The first three locations are at constant distances from the planar end wall, while the fourth is a constant distance from the contoured end wall. There is reasonably good agreement between the experimental and predicted data. Both show the minimum surface pressure on the suction surface occuring slightly beyond midchord.

Reference 4 stated that experimentally there was a 17-percent reduction in total pressure loss for the contoured end-wall case compared with the planar

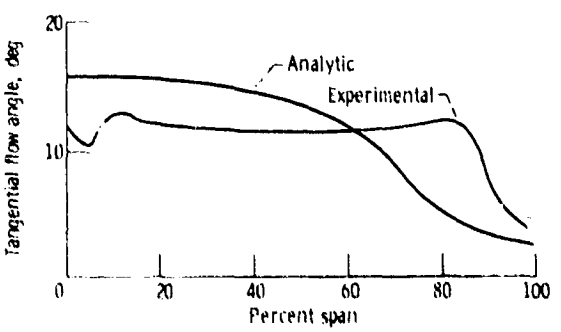

Figure 2. - Comparison of predicted and experimental mean flow angles one-third axial chord downstream of trailing edge. (Experimental data from ref. 4.)

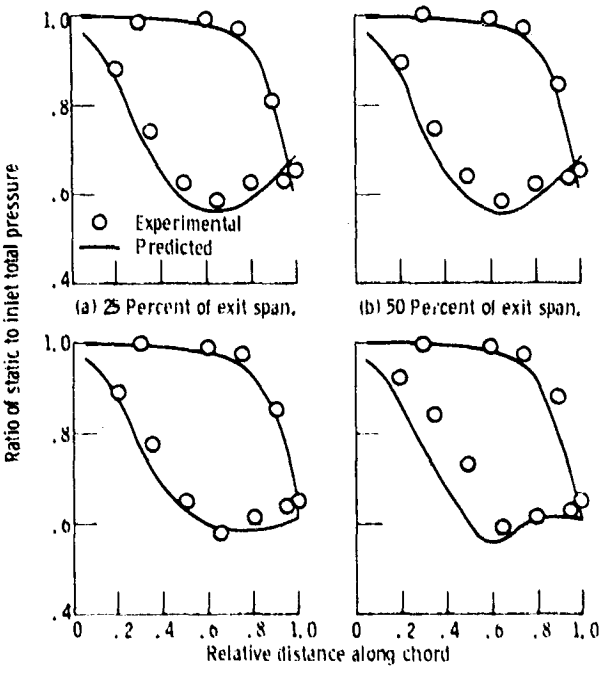

Figure 3. - Comparison of predicted and experimental blade surface pressures for planar cascade with contoured end wall. (Experimental data from ref. 4.)

end-wall case. The profile losses were about the same in the midspan region for both tests. The authors attribute the experimental improvement to reduced secondary flow losses. The quasi-three-dimensional analysis was done for each of the two experimental configurations. Analytically the profile losses for the contoured cascade were about the same as for the planar cascade. The calculated profile pressure loss was 1.2 percent, while the experimental profile pressure loss for the midspan region was 1.0 percent. The calculated total-pressure loss for the contoured cascade was 1.9 percent. The experimental total-pressure loss for the same configuration was also 1.9 percent. The calculated losses were based on boundary-layer growth. Any secondary loss not accounted for by boundary-layer growth should be added to the calculated loss.

Analysis of Effect of Contour Geometry on Stator Performance

A parametric analysis of contour geometry was undertaken to help understand why a contoured end wall results in improved performance. It was not expected that optimums resulting from this parametric analysis would hold for all stator designs, but it was felt that the trends would be applicable for stators of similar designs. While the blade design tested in the planar cascade and the stator design described in table I were both for the same application (the core turbine of an advanced energy efficient engine), they differed in several respects. The experimental stator had a higher turning angle, a higher axial aspect ratio, and a lower axial solidity. The experimental tests were done for a planar cascade while the parametric analysis was done for an annular cascade. The parametric analysis was done for a stator that was expected to benefit from the use of a contoured end wall, although the effect of stator design is discussed. The following table gives some characteristics of the stator, as well as the range of variables used in the parametric analysis.

Trailing edge angle, deg	74
Exit hub to tip radius ratio	0.86, 0.93
Mean axial solidity at exit	0.63
Ratio of chord to axial chord	2.0
Axial aspect ratio at exit, A	0.5
Aspect ratio at exit	0.25
Ratio of inlet to exit passage height, h	1.0 to 1.3
Uncontoured length, a, percent	0 to 71
Length of contoured portion of end-wall, b, percent	29 to 100
Upstream velocity ratio (cylindrical case), M^*	0.16
Downstream mean radius velocity ratio (cylindrical case), M^*	0.83
Contour shape	Variable

The flow rate was held constant as the contour geometry was varied. Since the downstream whirl changed with contour geometry, the downstream velocity changed for different contour geometries.

It was desired that the flow near the end wall not be accelerated too rapidly when the transition to the contour occurred. To facilitate this, the contour was constrained to have both zero curvature and zero slope at each end. For simplicity all contours were symmetric around their midpoint. A seventh order polynomial was used to meet the imposed constraints and allow the shape of the contour to be varied.

Effect of inlet to exit passage height. – Figure 4 compares the relative gain in efficiency as a function of the inlet to exit passage-height ratio. It can be seen from this figure that the maximum improvement in stator efficiency is approximately 0.8 percentage points. Since the efficiency of the uncontoured stator was 96.4 percent, the 0.8 percentage point gain in efficiency represents a 22 percent reduction in stator losses. The improvement in stator efficiency is due to both reduced profile loss and to reduced end-wall loss. The reduced profile loss contributes about two-thirds of the improvement, while the reduced end-wall loss contributes the remainder.

Because of the cross-channel pressure gradients, there was considerable uncertainty in the end-wall loss. The improvement in end-wall loss occurred across the end wall, and not just near the blade surfaces. There would not be a significant effect on the results if no averaging was done, and the end-wall loss was calculated using only the midchannel streamline data. The end-wall loss calculated using only the midchannel streamline was somewhat lower than the loss using the average of five streamlines.

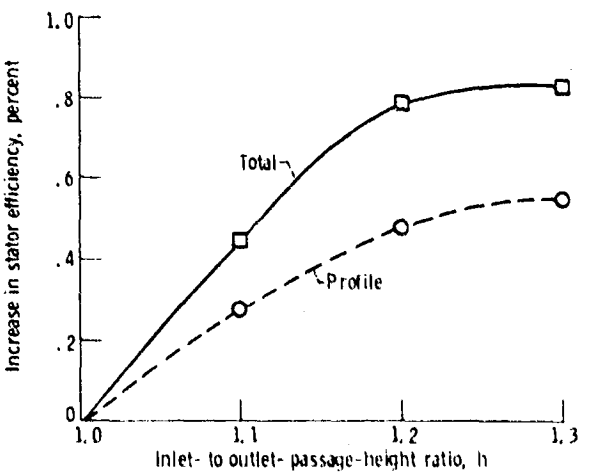

Figure 4. - Relative improvement in stator analytic efficiency as function of inlet- to outlet-passage-height ratio. (A = 0.5, a = 57%, b = 43%.)

The relative improvement in end-wall loss due to contouring was about the same for either method of calculating the results. If the midchannel loss was taken as the loss for the entire end wall, then the maximum gain in stator efficiency would still be over 0.7 percentage point.

The curves in figure 4 were stopped at a passage-height ratio of 1.3 because this height ratio resulted in near maximum efficiency gain. In addition, the higher passage-height ratios result in reduced tangential momentum. This occurred because the flow rate was held constant and the throat area increased with increased height ratios. At a passage-height ratio of 1.2 the average loss in momentum was about 2 percent, while at a ratio of 1.3 the loss increased to about 4 percent.

Figure 5 compares blade surface velocities for a cylindrical and a contoured end wall. Data are shown for the hub, mean, and tip. The contour begins at 57 percent of chord and ends at the trailing edge. The inlet to outlet passage-height ratio of 1.2 resulted in good efficiency gain without excessive loss of momentum. Most of the profile loss was due to boundary-layer growth on the suction surface, and figure 5 shows noticeably different suction-surface velocities for the two cases. Boundary-layer growth is inhibited by keeping a favorable pressure gradient along the blade for as long as possible. The contoured end wall has the peak surface velocity occur further aft for the hub and mean sections. This resulted in reduced boundary-layer growth. For the tip section there are two steep acceleration phases for the contoured end wall. At the end of the second acceleration the boundary layer was reduced relative to the cylindrical section. However, the rapid deceleration from the peak velocity to the trailing edge yielded rapid boundary-layer growth. This resulted in nearly the same profile loss for the contoured end wall at the tip, but the overall profile loss from hub to tip was lower for the contoured end-wall case. The reduction in end-wall loss due to the contour was the result of net axial reduction in boundary-layer growth on the hub and on the tip.

It was expected that the results shown in figure 4 would not be applicable to blades that had significantly different surface velocities than shown

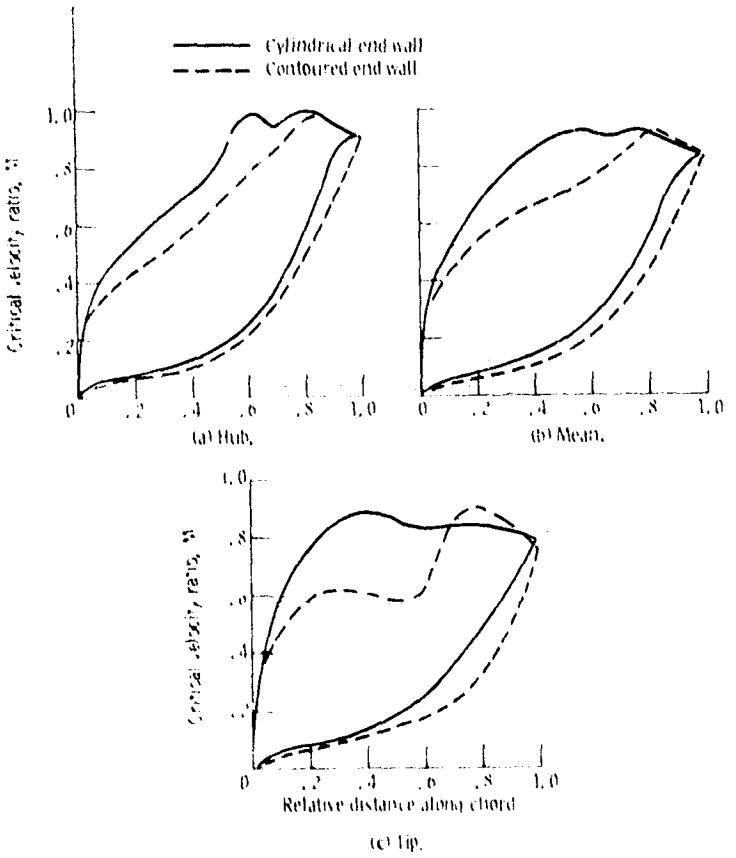

Figure 5. Comparison of blade surface velocities for cylindrical and contoured end walls. ($D_t = 1.2$, $A = 0.5$, $a = 5/3$, $b = 4/3$.)

in figure 5 for the cylindrical case. To check this, a different blade geometry was investigated. This blade was designed for a different application, but had about the same aspect ratio and turning angle. Figure 6 shows the blade surface velocities for the cylindrical end-wall design. In this design the peak suction surface velocity occurred at about 90 percent of chord. This differed from the cylindrical case shown in figure 5 where the peak suction surface velocity occurs near midchord. As a result of the peak suction-surface velocity occuring at 90 percent of chord, the alternative design began with lower velocity turning. When the effect of end-wall contouring was examined for the alternative design, the improvement was only about half the improvement for the configuration used in the parametric analysis.

Driving forces for secondary flows. – Figure 1 shows that most of the turning occurs in the first half of the axial distance. Figure 5 shows that the surface velocities are lower in this area for the contoured end-wall case. This results in a lower pressure difference across the passage and should result in reduced cross-channel flows near the end wall.

One additional benefit of end-wall contouring is the ability to modify the radial pressure gradient in an annular row of a turbine stator. If the gradient is reduced, the tendency for inward radial secondary flows is reduced. Figures 7 and 8 show the effect of end-wall contouring on the blade surface pressures. Figure 7 shows the ratio of a static to inlet total pressure as a function of the distance along the suction surface of the blades. The contoured case is for the same geometry as was used for the surface velocities shown in figure 5. Figure 7 also shows that the constant pressure curves are significantly different for the cylindrical and contoured end-wall cases. In the contoured end-wall case there is a smaller pressure gradient to drive radial inward secondary flows. Also, the area of the blade surface over which the gradients are predominately radial is less for the contoured end-wall case. Figure 8 makes

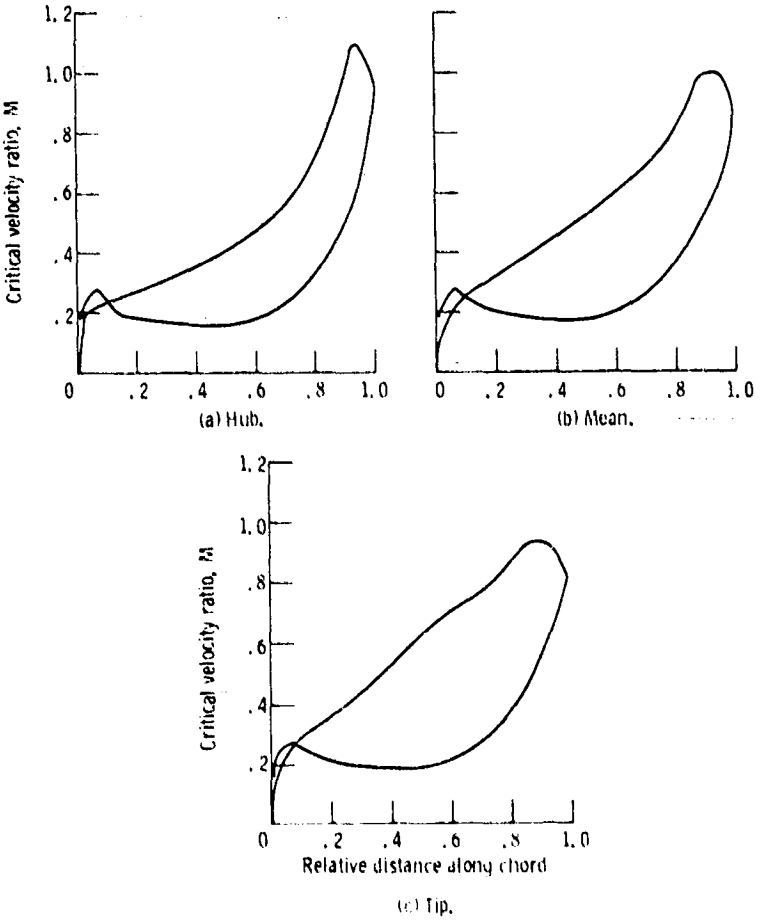

Figure 6. - Blade surface velocities for lightly loaded cylindrical stator.

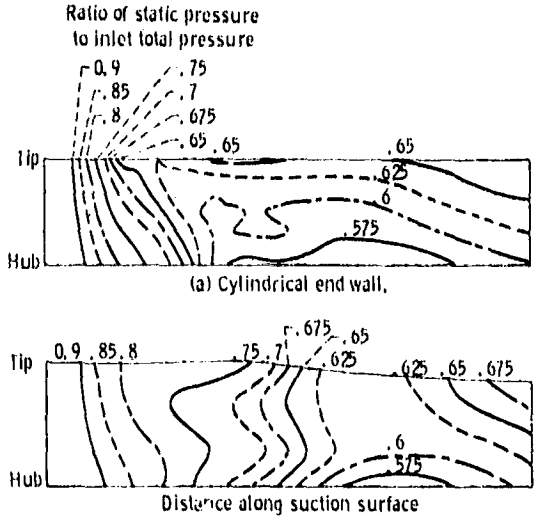

Figure 7. - Comparison of analytic pressure distribution along suction surfaces for cylindrical and contoured end walls. (h = 1.2, A = 0.5, a = 57%, b = 43%.)

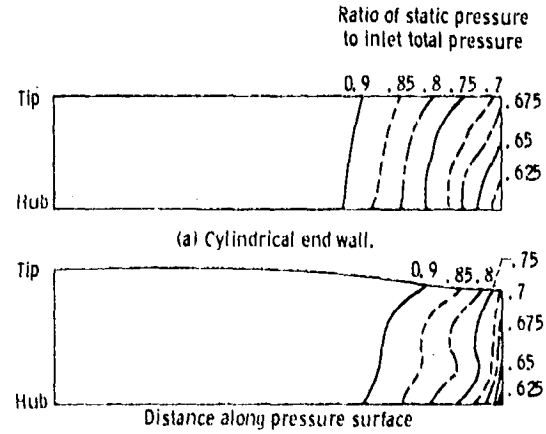

Figure 8. - Comparison of analytic pressure distributions along pressure surfaces for cylindrical and contoured end walls. (h = 1.2, A = 0.5, a = 57%, b = 43%.)

the same comparison except for the pressure surface. From this figure it can be seen that there is little difference in surface pressures on the pressure surface between the two cases.

Effect of contour length. – Figure 9 shows the effect of contour length on stator efficiency. Data are given for contours which end at the trailing edge. Results are shown for two inlet to outlet passage-height ratios. As the contour length decreases from a full chord to about half a chord, there is an improvement in stator efficiency for both passage-

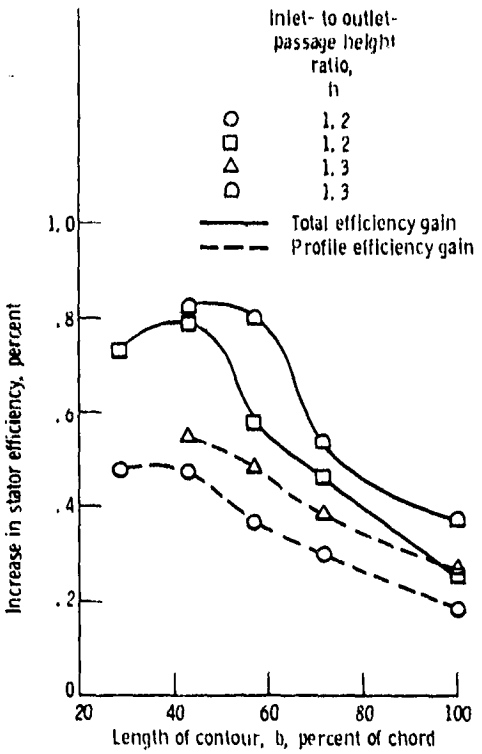

Figure 9. - Improvement in analytic efficiency for contours that terminate at end of passage.

height ratios. For shorter contour lengths there may be additional efficiency improvements, but they would be small. The iterations for individual data points were stopped when the uncertainty in the total loss was about 0.1 percentage point. Therefore, trends based on differences of this magnitude should not be considered significant. For the same height ratio, contours a full chord long have smaller passage areas in the region where the flow is turned rapidly than contours which begin near midchord. Contours which are a full chord long can be viewed as having a lower effective height ratio than those which begin at midchord. Therefore, from the results shown in figure 4 it was expected that the efficiency gain would be less for longer contours. Figure 5(c), shows that there is a tendency for the tip suction surface velocity to overshoot the trailing edge velocity for the contoured end-wall case. The peak suction-surface velocity occurs at about 80 percent of chord for a contour 43 percent of the chord long. From figure 9 it can be seen that there is no improvement in efficiency when the contour length is reduced from 43 to 29 percent of chord. For the shorter contour the peak velocity at the tip was higher because the rapid increase in surface velocity was further downstream in the passage. This higher peak velocity at the tip

leads to higher tip losses, which are not entirely overcome by improvements elsewhere.

Figure 9 does not show the tangential momentum associated with each case. There was a decrease in momentum as the contour length decreased. When the contour was the full passage length, the loss in momentum was less than 2 percent for both height ratios. For a height ratio of 1.2 the loss was about 2 percent, when the contour length was 43 percent or greater. When the contour was shortened to 29 percent of chord, the loss increased to about 8 percent. For a height ratio of 1.3 the loss was about 4 percent for contours that were 71, 57, and 43 percent of chord long. As either the height ratio increased or the contour was shortened, the throat area increased. Since the mass flow was held constant, the throat velocity decreased with increased throat area. This leads to lower downstream velocities, and consequently, lower tangential momentum.

Contour location. – The effect of placing the contour so that it terminated ahead of the trailing edge was investigated. By providing a cylindrical tip downstream of the contour, tangential momentum was maintained within 1 percent of the cylindrical end-wall case. Unfortunately, the efficiency gains were reduced. Figure 10 illustrates the effect of ending the contour before the trailing edge on stator efficiency. The decrease in stator efficiency does not seem to warrant placing the contour so that it ends before the trailing edge.

Effect of contour shape. – The contour shape was determined by specifying the slope at the midpoint of the contour. In the analysis, this slope was not varied in an arbitrary manner. The maximum slope used was the largest one for which the tip radius within the contour did not exceed the inlet tip radius. The minimum slope was the smallest one which did not result in more than the single inflection point at the contour midpont. The ratio of the midpoint slope to the slope calculated by dividing the change in tip radius by the contour axial length varied between 1.46 and 2.19. The effect of contour shape was investigated for the same contour configuration as was used for the results shown in figures 5, 7, and 8. Over the range of midpoint slopes the change in stator efficiency was less than 0.1 percentage point. This indicated that a fifth-order polynomial would be sufficient to describe the contour profile. The fifth-order polynomial has a fixed slope ratio of 1.88, which is about midway between the two slope ratios used to define the extremes of desirable contours.

Effect of radius ratio. – Based on the results given in reference 1 it was expected that a fairly low aspect ratio would be appropriate for the parametric analysis. The low aspect ratio would tend to result in stator designs with fairly high hub to tip radius ratios. To assess the effect of radius ratio on stator performance, a single point comparison was made. The results shown previously were obtained using a radius ratio of 0.86 at the stator exit. The effect of increasing this ratio to 0.93 was investigated. Two additional cases were run using the higher radius ratio. Both cases had the same aspect ratio and solidity as was used previously. The first case was for a cylindrical end wall, and the second case had the same contour geometry as the contoured end-wall case used for the results shown in figure 5, 7, and 8. The improvement in stator efficiency as a result of using the end-wall contour was about the same for the two radius ratios.

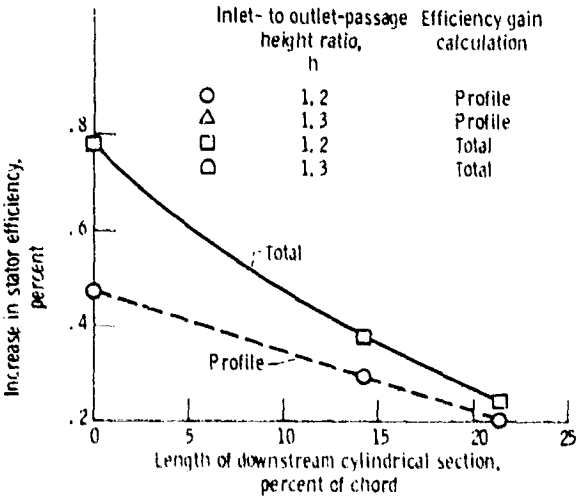

Figure 10. - Effect of terminating contour inside of passage on calculated stator efficiency. (h = 1.2, A = 0.5, b = 43%.)

Concluding Remarks

Reduced stator losses and improved overall efficiency in turbines with low aspect ratio blading have been achieved through contouring the stator outer wall. These performance gains were attributed to reduced velocities in the region of rapid turning which resulted in reduced boundary-layer growth and secondary flow losses. No comprehensive analyses were available in the literature, however, to describe and quantify the changes in flow characteristics that accompanied the geometric changes.

Consequently, a channel flow analysis was undertaken to provide a better understanding of end-wall contouring. The flow field in a variety of configurations was calculated using a combination of two-dimensional inviscid analyses and boundary-layer calculations. This approach resulted in a mapping of velocity and static pressure throughout

the stator passage, but could not determine the magnitude of cross-channel secondary flows on the blade surfaces and end walls. The output was therefore limited to calculated boundary-layer losses without secondary flow effects and the static-pressure field that provided the driving forces for secondary flows.

The result of this study substantially agreed with published experimental data in terms of trends for desirable contour geometries. On the basis of the calculated results, it appears that the performance improvement results from reduced velocities in the region of rapid turning. Low velocities in the region of rapid turning result in reduced boundary-layer growth. Also, the driving forces for secondary flows are reduced in this region, which leads to the expectation of reduced secondary losses. This was one of the conclusions from the published experimental data.

The results of this study are limited, but they provide insight into the loss characteristics of a turbine stator channel. Further understanding will be provided by three-dimensional computer codes as they become available.

Lewis Research Center
National Aeronautics and Space Administration
Cleveland, Ohio, March 17, 1981

References

1. Deich, M. E.; et al: Method of Increasing the Efficiency of Turbine Stages and Short Blades. Translation No. 2816, Associated Electrical Industries (Manchester) Limited, 1960.
2. Ewen, J. S.; Huber, F. W.; and Mitchell, J. P.: Investigation of the Aerodynamic Performance of Small Axial Turbines. ASME Paper 73-GT-3, Apr. 1973.
3. Morris, A. W. H.; and Hoare, R. G.: Secondary Loss Measurements in a Cascade of Turbine Blades with Meridional Wall Profiling. ASME Paper 75-WA/GT-13, Nov. 1975.
4. Kopper, F. C.; Milano, R.; and Vanco, M.: An Experimental Investigation of Endwall Profiling in a Turbine Vane Cascade. AIAA Paper 80-1089, July 1980.
5. Katsanis, Theodore; and McNally, William D.: Revised Fortran Program for Calculating Velocities and Streamlines on the Hub-Shroud Midchannel Stream Surface of an Axial-, Radial-, or Mixed-Flow Turbomachine or Annular Duct. Vol. I—User s Manual. NASA TN D-8430, 1977.
6. Katsanis, Theodore: Fortran Program for Calculating Transonic Velocities on a Blade-to-Blade Stream Surface of a Turbomachine. NASA TN D-5427, 1969.
7. McNally, William D.: Fortran Program for Calculating Compressible Laminar and Turbulent Boundary Layers in Arbitrary Pressure Gradients. NASA TN D-5681, 1970.
8. Goldman, Louis J.; and McLallin, Kerry L.: Cold-Air Annular-Cascade Investigation of Aerodynamic Performance of Cooled Turbine Vanes. I—Facility Description and Base (Solid) Vane Performance. NASA TM X-3006, 1974.
9. Stewart, Warner L.: Analysis of Two-Dimensional Compressible-Flow Loss Characteristics Downstream of Turbomachine Blade Rows in Terms of Basic Boundary-Layer Characteristics. NACA TN-3515, 1955.

END

DATE

FILMEI

EB 24 1982